Improvement of Electrical Properties of $Ba_{0.7}Sr_{0.3}TiO_3$ Capacitors With an Inserted Nano-Cr Interlayer

Chia-Cheng Ho, *Student Member, IEEE*, Bi-Shiou Chiou, *Senior Member, IEEE*, and Li-Chun Chang

***Abstract*—The metal–insulator–metal (MIM) capacitors were prepared with $Ba_{0.7}Sr_{0.3}TiO_3$/Cr/$Ba_{0.7}Sr_{0.3}TiO_3$ (BST/Cr/BST) dielectric and Pt electrode. The multilayer BST/Cr/BST was sputtered onto Pt/Ti/SiO_2/Si substrate. The presence of nano-Cr interlayer affects the electrical properties of the capacitors. The temperature coefficient of capacitance (TCC) of capacitors with 2 nm Cr is about 69% of that of capacitors without Cr. In a previous work, the formation of the TiO_2 secondary phase was found after the BST/Cr/BST dielectrics were annealed at 1023 K in O_2 atmosphere for 1 h. It is suggested that the nano-Cr interlayer as a catalyst leads to the TiO_2 formation during the annealing in O_2 atmosphere. The negative value of TCC of BST can be compensated by the positive TCC of TiO_2, and the temperature stability in the dielectric constant can be realized for capacitors with nano-Cr interlayer. The voltage stability of BST is also improved with the insertion of nano-Cr interlayer, and the quadratic coefficient in voltage coefficient of capacitance (VCC) of Pt/BST/Cr(2 nm)/BST/Pt is about 30% of that of the BST capacitor without Cr. The effects of Cr thickness on TCC, VCC, dissipation factor, and leakage current density of Pt/BST/Cr/BST/Pt parallel plate capacitors are investigated.**

***Index Terms*—$Ba_{0.7}Sr_{0.3}TiO_3$/Cr/$Ba_{0.7}Sr_{0.3}TiO_3$ (BST) capacitor, dissipation factor, nano-Cr interlayer, voltage coefficient of capacitance (VCC).**

I. Introduction

In THE PAST decades, improvements in circuit performance and cost per function have been pursued by shrinking device geometries. In order to keep the storage capacitance, $Ba_xSr_{1-x}TiO_3$ dielectrics are extensively investigated for applications in the high-density dynamic random access memories (DRAM) and the capacitors of the analog/mixed circuit. The high charge storage density, the low leakage current, high breakdown field, and high time-dependent dielectric breakdown (TDDB) [1]–[3] of BST are attractive for use in DRAM and the analog/mixed-signal circuit. However, the stability of the BST dielectric constant becomes a major concern while the applied voltage and/or operating temperature vary. The quadratic voltage coefficient of capacitance (VCC) is a critical factor for the capacitor in DRAM and the analog/mixed-signal circuit [4], [5]. Besides, the dielectric constant of BST varies with the operating temperature [6]–[9], which affects the precise capacitance.

Previously, nanoferroelectric-based core-shell particles have been used for improving the characteristics of the ferroelectric dielectrics [10], and nanocomposite capacitor shows the promising dielectric properties with the ceramic fillers [11]. Our previous work [6]–[8] shows that parallel plate capacitors with an inserted nano-Cr interlayer exhibit lower leakage current and more temperature stable in the dielectric constant. However, there are few papers regarding the stabilities of the capacitors with the nano-Cr interlayer as the operation temperature and the applied voltage change. Besides, the formation of TiO_2 film was found in the annealed specimens with the nano-Cr interlayer. In this study, the effects of the Cr thickness on the temperature and voltage stability of the dielectric behaviors of Pt/BST/Cr/BST/Pt capacitors are investigated.

Manuscript received June 16, 2007; revised January 6, 2008. This work was supported by the National Science Council, Taiwan, under Contract NSC 95-2221-E-009-085. The review of this paper was arranged by Associate Editor B. Yu.

C.-C. Ho and B.-S. Chiou are with the Department of Electronics Engineering, National Chiao-Tung University, Hsinchu 300, Taiwan, R.O.C. (e-mail: doubles.ee89g@nctu.edu.tw; bschiou@mail.nctu.edu.tw).

L.-C. Chang is with the Department of Materials Engineering, Mingchi University of Technology, Taipei 243, Taiwan, R.O.C. (e-mail: lcchang@edirect168.com).

Color versions of one or more of the figures in this paper are available online at http://ieeexplore.ieee.org.

Digital Object Identifier 10.1109/TNANO.2008.920201

II. Experimental Procedures

Specimens of Pt/$Ba_{0.7}Sr_{0.3}TiO_3$/Cr/$Ba_{0.7}Sr_{0.3}TiO_3$/Pt MIM capacitors were employed. The starting p-type Si (1 0 0) wafers were cleaned by the standard Radio Corporation of America (RCA) cleaning process. After cleaning, a 100-nm-SiO_2 films were grown on the Si substrate by the dry-oxidation in 1273 K for 30 min. A 10-nm-Ti films were sputtered onto the SiO_2 layer. The bottom electrodes, 100-nm-thick Pt films, were dc sputtered at room temperature. The $Ba_{0.7}Sr_{0.3}TiO_3$ (BST) films were then deposited onto Pt electrodes using an RF magnetron sputtering at a substrate temperature of 625 K. The sputtering chamber was evacuated to a base pressure of 1×10^{-5} torr. During the deposition of BST films, a constant pressure of 5×10^{-3} torr was maintained by a mixture of argon and oxygen at 9 and 3 sccm, respectively. The RF power for the deposition of both the first and second BST layers was 120 W (power density was 2.7 W/cm^2), and the total thickness of BST films was about 300 nm. Chromium films with various thicknesses (2, 5, 10, and 15 nm) were deposited at a dc power of 100 W after the deposition of the first BST films without the vacuum broken. The thickness of Cr films was monitored with a quartz crystal and a controller. The second BST layers were then deposited. The BST/Cr/BST/Pt specimens were annealed at 1023 K in O_2 for 1 h, and then were bombarded by O_2 plasma for 10 min before the deposition of the top Pt electrode.

The high-resolution transmission microscopy (HRTEM) (JEM-3000 F, JEOL Ltd., Japan) was employed to observe

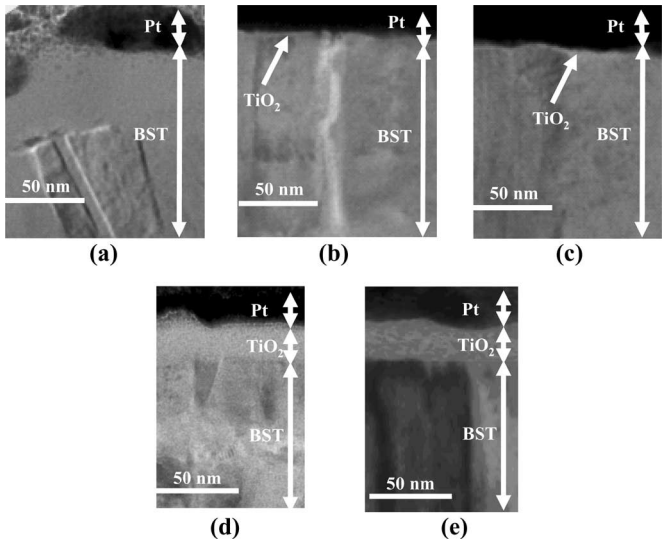

Fig. 1. Cross-sectional image on the Pt/BST/Cr/BST/Pt specimen with a Cr thickness of the following. (a) 0 nm. (b) 2 nm. (c) 5 nm. (d) 10 nm. (e) 15 nm.

the structure of specimens. The cross-sectional TEM specimen was prepared using the focused ion beam (FIB) system (Nova 200, FEI company, Japan). An LCR meter (HP-4285, Hewlett Packard Company, USA) was employed to measure the dielectric constant and dissipation factor of the samples in the temperature range from 298 K to 398 K. A semiconductor parameter analyzer (HP4155B, Hewlett Packard Company, USA) was employed to measure the leakage current, and the activation energies were obtained in the temperature range from 298 K to 423 K.

III. Results and Discussion

Fig. 1(a)–(e) are the cross-sectional HRTEM images of BST dielectric structure. Specimens with mono BST layer annealed in O_2 atmosphere for 1 h exhibit the uniform microstructure and no thin layer formation, as shown in Fig. 1(a). Other BST/Cr/BST specimens indicate the formation of a thin layer on the top BST layer, as shown Fig. 1(b)–(e). Our previous work suggests that a β-TiO_2 secondary phase is formed after the BST/Cr/BST dielectrics are annealed in O_2 for 1 h [7], [8]. Hence, the thin layer on top of the BST is TiO_2. However, the formation of TiO_2 is not clear now. The possible mechanism is that Cr layer as the catalyst leads to the TiO_2 formation during the annealing in O_2 atmosphere. In the case of mono BST annealing in O_2 atmosphere, there is no TiO_2 formation for mono BST dielectric, as shown in Fig. 1(a). In our previous work [6], the second phase in BST/Cr(2 nm)/BST annealed in air was also found, but no second phase was appeared for BST/Cr(2 nm)/BST annealed in N_2 atmosphere. All agree with the formation of TiO_2 from the catalyst (Cr). Though the created new compounds of BST films are possible, Cr^{+3} (0.130 nm) is difficult to replace Ti^{+4} (0.145 nm) in the pervoskite structure, and the shift of Ti binding energy is not obvious [8].

Fig. 2 shows the temperature dependence of the dielectric constant of specimens with various Cr thicknesses (t_{Cr}) as function of the applied electric field at an oscillation voltage of 0.1 V and a measuring frequency of 100 kHz. The dielectric constant decreases as t_{Cr} increases. Comparing with mono-BST capacitor ($\varepsilon \sim 456$), the dielectric constant (ε) decreases to 371 for specimens with 2-nm-Cr layer, as exhibited in Fig. 2 and summarized in Table I. The temperature coefficient of capacitance (TCC) is defined as

$$\mathrm{TCC} = \frac{C_T - C_{T_r}}{(T - T_r) \times C_{T_r}} \tag{1}$$

where *T* is the temperature of interest (398 K in this study), T_r is the temperature of reference (298 K in this study), and C_T and C_{Tr} are the capacitances at zero-bias measured at *T* and T_r, respectively. The TCCs of the specimens are listed in Fig. 2. A TCC of -0.5×10^{-3}/K is obtained for capacitors with 2 nm Cr as compared to that of -1.6×10^{-3}/K for capacitors without nano-Cr interlayer, while positive TCCs are obtained for specimens with thicker t_{Cr} interlayer of 10 nm. The BST employed in this study has a negative TCC, while the TiO_2 exhibits a positive TCC [12]. It is argued that the positive TCC of the TiO_2 compensates the negative TCC of BST. The TiO_2 formation resulted from the presence of Cr interlayer [8] improves the temperature stability of the dielectric constant of BST films. Fig. 3 gives the TiO_2 thickness ($t_{\mathrm{TiO_2}}$) of specimens from Fig. 1(b)–(e). On the basis of $t_{\mathrm{TiO_2}}$, the TiO_2 dielectric constants ($\varepsilon_{\mathrm{TiO_2}}$) based on serial capacitor model were calculated with the following equation

$$\varepsilon_{\mathrm{TiO_2}} = \frac{t_{\mathrm{TiO_2}} C \varepsilon_{\mathrm{BST}}}{a\varepsilon_{\mathrm{BST}} - t_{\mathrm{BST}} C} \tag{2}$$

where *C* is the measured capacitance, *a* is the electrode area, and $\varepsilon_{\mathrm{TiO_2}}$ ($t_{\mathrm{TiO_2}}$) and $\varepsilon_{\mathrm{BST}}$ (t_{BST}) are the dielectric constant (thickness) of TiO_2 and BST, respectively. The estimated $\varepsilon_{\mathrm{TiO_2}}$, as shown in Fig. 3, is almost keep constant, and the average value is 21.6, which is consistent with [13].

The nano-Cr interlayer also improves the voltage stability of the dielectric constant of BST capacitor. The voltage stability of the capacitors can be expressed in terms of the VCC obtained from a second-order polynomial equation

$$C(V) = C_o(AV^2 + BV + 1) \tag{3}$$

where C_o is the capacitance at zero-bias, and *A* and *B* are the quadratic and linear voltage coefficients of the capacitance, respectively. On the basis of Fig. 2, the VCCs of specimens are calculated and summarized in Table I. The BST/Cr/BST dielectric decreases the absolute value of the quadratic coefficient (*A*) from $5.93 \times 10^{-3}/\mathrm{V}^2$ of the mono-BST dielectric to $1.78 \times 10^{-3}/\mathrm{V}^2$ of BST/Cr(2 nm)/BST dielectric and $1.03 \times 10^{-3}/\mathrm{V}^2$ of BST/Cr(15 nm)/BST dielectric at 298 K. Among all measuring temperatures, BST/Cr/BST dielectric shows more voltage stable than the mono-BST dielectric, as indicated in Table I.

The dissipation factor, as shown in Fig. 4, decreases initially, and then, increases as t_{Cr} increases. The BST/Cr(2 nm)/BST dielectric shows the smallest dissipation factor of 0.023 as compared to the 0.028 of mono-BST dielectric. Fig. 5(a) exhibits the leakage current density (*J*) versus electric field (*E*) of the

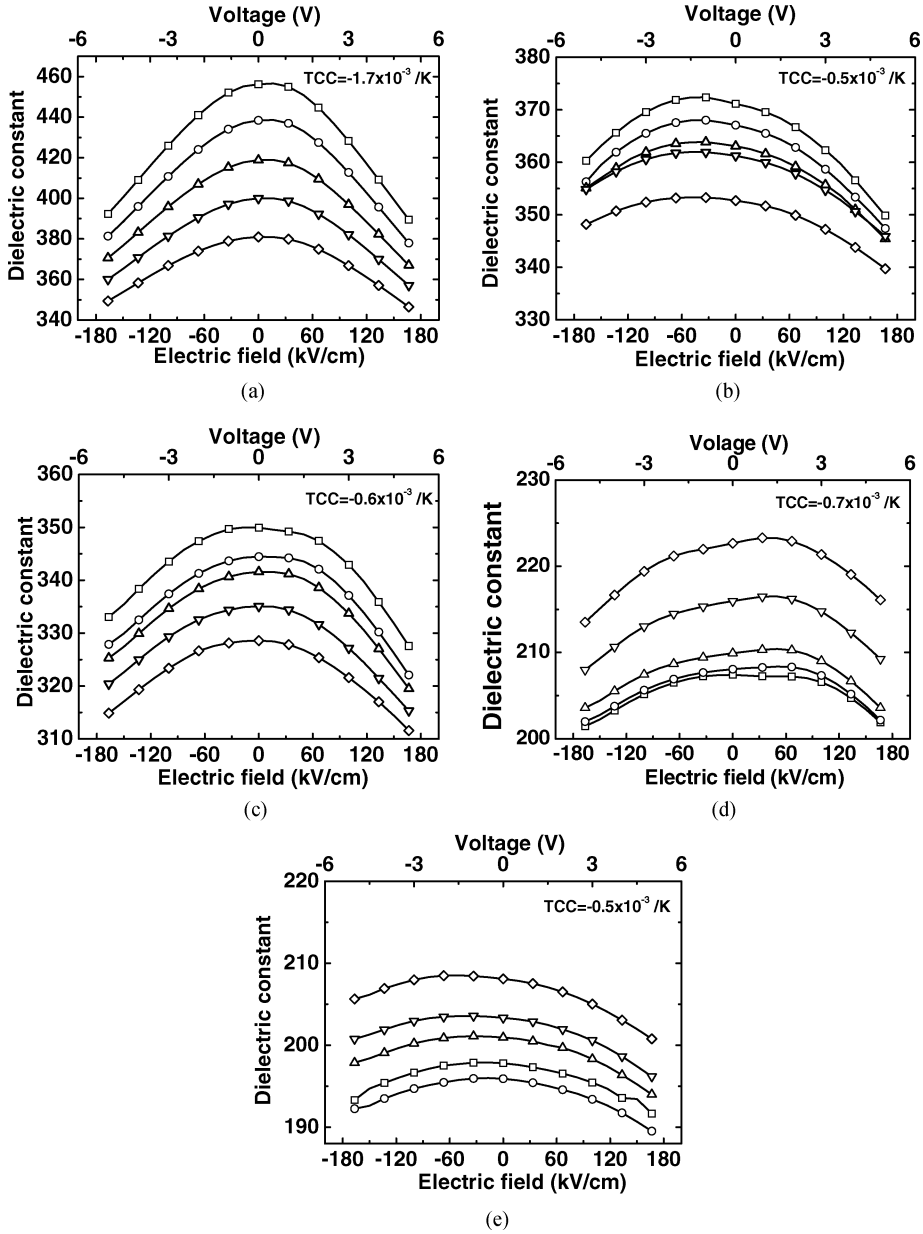

Fig. 2. Electric field dependence of the 100 kHz dielectric constant of the following as the function of the temperature. (a) Mono-BST. (b) BST/Cr(2mn)/BST. (c) BST/Cr(5 nm)/BST. (d) BST/Cr(10 nm)/BST. (e) BST/Cr(15 nm)/ BST. The TCC from 298 K to 398 K are indicated. The temperatures of measurement are 298 K (□), 323 K (○), 348 K (△), 373 K (▽), and 398 K (◇).

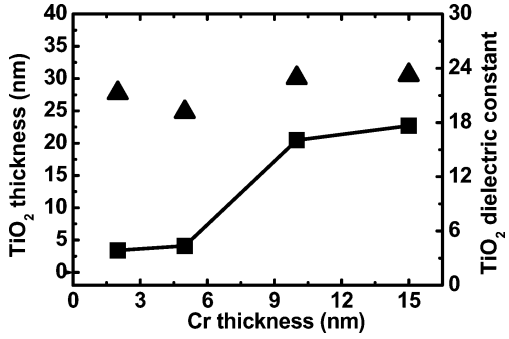

Fig. 3. TiO_2 thickness (■) from TEM image and the calculated dielectric constant of TiO_2 (▲) versus the Cr thickness.

capacitors at 298 K. Capacitors with $t_{\mathrm{Cr}} = 2$ and 5 nm show lower leakage current at electric fields below 50 kV/cm than other capacitors. A linear relationship is obtained on the Ln(*J*/*E*) and Ln(J/T^2) versus $E^{0.5}$, as shown in Fig. 5(b) and (c), respectively, which suggests Schottky emission (SE) or Poole–Frenkel (PF) emission mechanisms [14], [15]. The leakage current densities of the two conduction mechanisms are expressed as follows:for SE:

$$\mathrm{Ln}\left(\frac{J_{\mathrm{SE}}}{A^{*}T^{2}}\right) = \frac{\beta_{\mathrm{SE}}E^{0.5} - \varphi_{\mathrm{SE}}}{k_B T} \tag{4}$$

for PF:

$$\mathrm{Ln}\left(\frac{J_{\mathrm{PF}}}{E}\right) = \frac{\beta_{\mathrm{PF}}E^{0.5} - \varphi_{\mathrm{PF}}}{k_B T} \tag{5}$$

TABLE I
VOLTAGE COEFFICIENT OF CAPACITANCE (VCC)$^{\#}$ AT VARIOUS TEMPERATURES OF Pt/BST/Cr/BST/Pt CAPACITOR WITH VARIOUS Cr THICKNESSES (t_{Cr})

t_{Cr} (nm)	Voltage coefficient of capacitance (VCC$^{\#}$)					
		298 K	323 K	348 K	373 K	398 K
0	ε	456	438	419	400	381
	A (10^{-3} /V^2)	-5.93	-5.50	-4.89	-4.22	-3.53
	B (10^{-3} /V)	0.19	0.08	-0.13	-0.16	-0.33
2	ε	371	367	363	361	353
	A (10^{-3} /V^2)	-1.78	-1.67	-1.45	-1.20	-1.01
	B (10^{-3} /V)	-3.05	-2.83	-2.83	-2.60	2.42
5	ε	350	344	342	335	329
	A (10^{-3} /V^2)	-2.31	-2.36	-2.31	-2.12	-1.90
	B (10^{-3} /V)	-0.91	-0.83	-1.02	-1.25	-0.92
10	ε	207	208	209	216	222
	A (10^{-3} /V^2)	-1.11	-1.18	-1.18	-1.40	-1.45
	B (10^{-3} /V)	0.70	0.78	0.78	1.02	1.39
15	ε	198	196	201	203	208
	A (10^{-3} /V^2)	-1.03	-1.02	-1.00	-0.99	-0.96
	B (10^{-3} /V)	-0.95	-1.19	-1.72	-2.07	-2.32

#: $C(V)=C_o(AV^2+BV+1)$, where A and B are the quadratic and linear voltage coefficients of the capacitance, respectively.

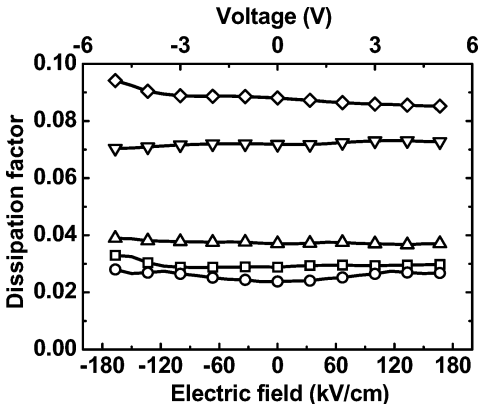

Fig. 4. Dissipation factor as the function of the electric field of BST/Cr/BST with various Cr thicknesses (t_{Cr}). (□), 0 nm; (○), 2 nm; (△), 5 nm; (▽), 10 nm; and (◇), 15 nm.

where $\beta_{\mathrm{SE}} = (e^3/4\pi\varepsilon_0\varepsilon_d)^{0.5}$, A^* is the effective Richardson's constant (120 A/cm^2/K^2), ϕ_{SE} is the potential barrier height at the surface, ε_0 is the dynamic dielectric constant of free space, ε_d is the dynamic relative dielectric constant in the infrared region, e is the unit charge, k_B is Boltzmann's constant, T is the absolute temperature, E is the external electric field, $\beta_{\mathrm{PF}} = (e^3/\pi\varepsilon_0\varepsilon_d)^{0.5}$, and ϕ_{PF} is the potential barrier height of trap potential well. The PF transport mechanism is a result of the lowering of the barrier height of traps in the dielectrics. The conduction mechanisms of metal/BST/metal capacitors are usually interpreted as SE at lower electric fields and PF emission at higher fields [1]. The dynamic relative dielectric constant can be inferred from n^2, where n is the refractive index. Therefore, the dynamic relative dielectric constant of BST films is about 4 [16].

The dashed lines in Fig. 5(b) and (c) are the PF and SE fittings, respectively. The slope of the Ln(J/E) and Ln(J/T^2) versus $E^{0.5}$ curve, as summarized in Table II, is β/k_BT. Both β_{SE} and β_{PF} are calculated and listed in Table II for comparison. The β values obtained in this study are closer to β_{SE} or β_{PF}, and this suggests that the dominant mechanism for charge carriers to transport is SE or PF emission in the different applied electric field. The PF fitting regions of the various Cr thicknesses (t_{Cr}) showing PF behaviors are above 53 kV/cm ($t_{\mathrm{Cr}} = 0$ nm), 37 kV/cm ($t_{\mathrm{Cr}} =$ 2 nm), 35 kV/cm ($t_{\mathrm{Cr}} = 5$ nm), 120 kV/cm ($t_{\mathrm{Cr}} = 10$ nm), and 125 kV/cm ($t_{\mathrm{Cr}} = 15$ nm). Lower values of PF boundary are obtained for BST specimens containing Cr interlayer ($t_{\mathrm{Cr}} = 2$ nm and $t_{\mathrm{Cr}} = 5$ nm). Our previous work [1] suggests the more oxygen vacancies and the higher interfacial space charge concentration, the smaller is the electric field boundary of SE/PF. It is suggested these defect appeared between $Ba_xSr_{1-x}TiO_3$ and TiO_2. Especially for the thin TiO_2 layer for the specimens of the BST/Cr(2 nm)/BST and BST/Cr(5 nm)/BST, the effects

TABLE II
β_{SE}, β_{PF}, ACTIVATION ENERGY (E_a), AND β EXTRACTED FROM CURVE FITTING (SLOPE: $\beta/k_B T$) OF THE SE OR PF EMISSION MECHANISM* OF Pt/BST/Cr/BST/Pt CAPACITOR WITH VARIOUS Cr THICKNESSES (t_{Cr})

t_{Cr} (nm)	β_{SE} (10^{-24})	β_{PF} (10^{-24})	β (10^{-24}) Fitting in the electric field range	E_a (eV.)
0	3.03	6.07	11.06 (PF) 53 kV/cm —— 200 kV/cm	0.039
2	3.03	6.07	11.84 (PF) 37 kV/cm —— 200 kV/cm	0.064
5	3.03	6.07	10.02 (PF) 35 kV/cm —— 200 kV/cm	0.049
10	3.03	6.07	4.05 (SE) 6.37 (PF) 58 V/cm —— 120 kV/cm —— 200 kV/cm	0.028
15	3.03	6.07	4.84 (SE) 6.11 (PF) 50 kV/cm —— 125 kV/cm —— 200 kV/cm	0.016

* SE emission mechanism: $Ln(J_{SE}/A^*/T^2) = (\beta_{SE}E^{0.5} - \phi_{SE})/(k_B T)$
PF emission mechanism: $Ln(J_{PF}/E) = (\beta_{PF}E^{0.5} - \phi_{PF})/(k_B T)$.

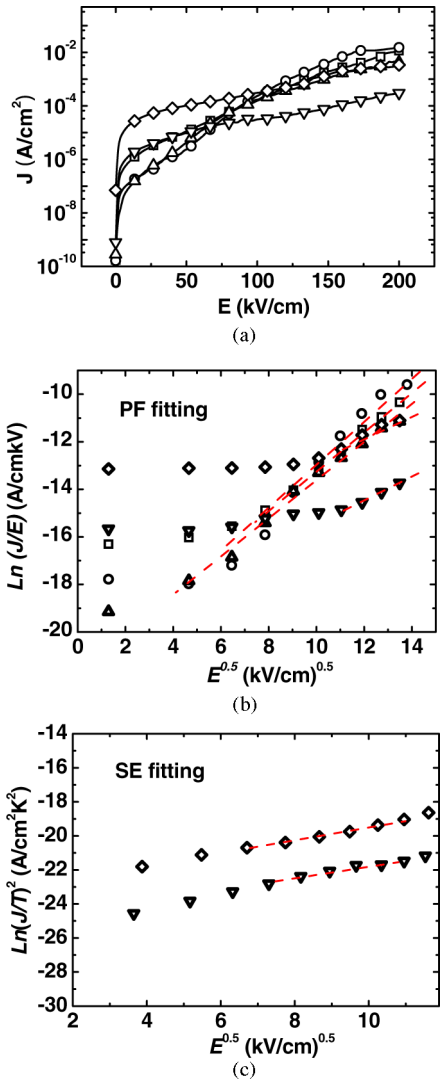

Fig. 5. (a) Leakage current density (J) versus electric field (E); (b) PF emission plot of $\mathrm{Ln}(J/E)$ versus $E^{0.5}$; (c) SE plot of $\mathrm{Ln}(J/T^2)$ versus $E^{0.5}$ of specimens are of BST/Cr/BST with various Cr thicknesses (t_{Cr}). (□), 0 nm; (○), 2 nm; (△), 5 nm; (▽), 10 nm; and (◇), 15 nm. The dashed lines are PF or SE fitting.

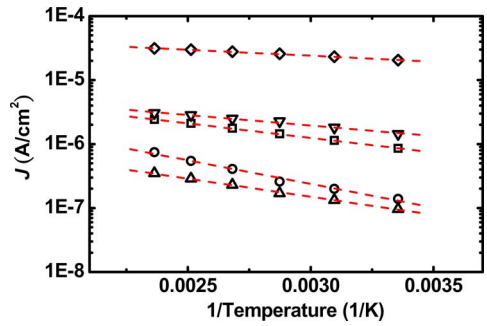

Fig. 6. Arrhenius plots of leakage current of BST/Cr/BST with various Cr thicknesses (t_{Cr}). (□), 0 nm; (○), 2 nm; (△), 5 nm; (▽), 10 nm; and (◇), 15 nm.

of the oxygen vacancies and the interfacial space charges on the leakage current are comparatively obvious.

Fig. 6 shows the Arrhenius plot of leakage currents from 298 K to 423 K. The activation energies of hopping electrons, calculated on the basis of Fig. 6 and exhibited in Table II, are 0.039 eV ($t_{Cr} = 0$ nm), 0.064 eV ($t_{Cr} = 2$ nm), 0.049 eV ($t_{Cr} = 5$ nm), 0.028 eV ($t_{Cr} = 10$ nm), and 0.016 eV ($t_{Cr} = 15$ nm). The specimens with $t_{Cr} = 2$ nm and 5 nm have higher activation energies. It could be because some defects could trap the charges to reduce the leakage current, but the thermal excitation of the trapped charge from one site to the other dominates the transport in the films [17], [18]. The reason may increase the activation energies of capacitors with $t_{Cr} = 2$ and 5 nm. Though the dielectric constant decreases with the increase of t_{Cr}, the BST specimen with 2-nm-Cr interlayer shows smaller leakage current, lower dissipation factor, and better temperature and voltage stabilities.

IV. CONSLUSION

MIM capacitors of Pt/BST/Cr/BST/Pt are investigated in this study. A TiO_2 film was formed after the BST/Cr/BST dielectric is annealed at 1023 K in O_2 atmosphere. The implementation of 2 nm Cr improves the dissipation factor, voltage stability,

temperature stability, and leakage current of the BST dielectrics. A dissipation factor of 0.023 at 100 kHz is obtained for BST/Cr (2 nm)/BST dielectric as compared to that of 0.028 for mono-BST dielectric. A TCC of -0.5×10^{-3}/K from 298 K to 398 K is obtained for BST/Cr(2 nm)/BST dielectric as compared to that of -1.6×10^{-3}/K for mono-BST dielectric. The improvement of the dielectric behaviors of the BST/Cr/BST is attributed to the formation of TiO_2 layer after the annealing. Besides, among all measuring temperatures, the BST/Cr/BST dielectric also shows more voltage stable than the mono-BST dielectric. The leakage current fittings show BST specimens containing Cr interlayer ($t_{\mathrm{Cr}} = 2$ and 5 nm) show lower values of PF boundary. The more oxygen vacancies and the higher interfacial space charge concentration, the smaller is the electric field boundary of SE/PF.

REFERENCES

[1] D. C. Shye, B. S. Chiou, M. J. Lai, C. C. Hwang, C. C. Jaing, J. S. Chen, M. H. Cheng, and H. C. Cheng, "Low temperature radio-frequency-sputtered (Ba,Sr)TiO_3 films on Pt/TiN/Ti/Si substrate with various oxygen/argon mixing ratios," *J. Electrochem. Soc.*, vol. 150, no. 2, pp. F20–F27, Feb. 2003.

[2] D. C. Shye, B. S. Chiou, M. W. Kuo, J. S. Chen, B. C. S. Chou, C. C. Jaing, M. F. Wu, and H. C. Cheng, "Dependence of polarization on temperature coefficient resistance of (Ba,Sr)TiO_3 thin films posted-treated by RTA," *Electrochem. Solid-State*, vol. 6, no. 4, pp. G55–G58, Apr. 2003.

[3] J. W. Liou and B. S. Chiou, "Analysis of the dielectric characteristics for polycrystalline $Ba_{0.65}Sr_{0.35}TiO_3$ (I)-frequency dependence in the paraelectric state," *J. Mater. Sci.: Mater. Electron.*, vol. 11, no. 8, pp. 637–643, Nov. 2000.

[4] S. J. Kim, B. J. Cho, M. F. Li, S. J. Ding, C. Zhu, M.B. Yu, B. Narayanan, A. Chin, and D. K. Kwong, "Improvement of voltage linearity in high-*k* MIM capacitors using HfO2-SiO2 stacked dielectric," *IEEE Electron Device Lett.*, vol. 25, no. 8, pp. 538–540, Aug. 2004.

[5] K. S. Tan, S. Kiriake, M. Dewit, J. W. Fattaruso, C.Y. Tsay, W. E. Matthews, and R. K. Hester, "Error correction techniques for high-performance differential A/D convertes," *IEEE J. Solid-State Circuits*, vol. 25, no. 6, pp. 1318–1327, Dec. 1990.

[6] C. C. Ho, B. S. Chiou, L. C. Chang, C. C. Chou, B. H. Liou, and C. C. Yu, "Thermal stability and electric properties of $Ba_{0.7}Sr_{0.3}TiO_3$ parallel plate capacitor with nano-Cr interlayer," *Surf. Coat. Techol.*, vol. 201, no. 7, pp. 4163–4167, Dec. 2006.

[7] C. C. Ho, B. S. Chiou, and L. C. Chang, "Thickness effects on electrical characteristics of $Ba_{0.7}Sr_{0.3}TiO_3$ capacitors with nano-Cr interlayer," *Appl. Phys. Lett.*, vol. 90, no. 13, pp. 132906-1–132906-3, Mar. 2007.

[8] C. C. Ho, B. S. Chiou, and L. C. Chang, "Microstructure evolution and dielectric properties of $Ba_{0.7}Sr_{0.3}TiO_3$ parallel plate capacitor with Cr interlayer," *Surf. Coat. Techol.*, vol. 202, no. 4–7, pp. 768–773, Dec. 2007.

[9] M. W. Kuo, D. C. Shye, B. S. Chiou, J. S. Chen, and H. C. Cheng, "Effects of thermal stabilities for the ultra thin chromium layers applied on (Ba,Sr)TiO_3 thin films," *Integr. Ferroelectr.*, vol. 61, pp. 183–187, 2004.

[10] C. Huber, C. Elissalde, V. Hornebecq, S. Mornet, M. Treguer-Delapierre, F. Weill, and M. Maglione, "Nano-ferroelectric based core-shell particles: towards tuning of dielectric properties," *Ceram. Int.*, vol. 30, no. 7, pp. 1241–1245, 2004.

[11] J. J. Si, H. Ono, K. Uchida, S. Nozaki, H. Morisaki, and N. Itoh, "Correlation between the dielectric constant and porosity of nanoporous silica thin films deposited by the gas evaporation technique," *Appl. Phys. Lett.*, vol. 79, no. 19, pp. 3140–3142, Nov. 2001.

[12] A. G. Cockbain and P. J. Harrop, "The temperature coefficient of capacitance," *J. Phys. D Appl. Phys.*, vol. 1, no. 9, pp. 1109–1115, 1968.

[13] R. Singh, S. Alamgir, and R. Sharangpani, "Deposition of high dielectric constant materials by dual spectral source assisted metalorganic chemical vapor deposition," *Appl. Phys. Lett.*, vol. 67, no. 26, pp. 3939–3041, Dec. 1995.

[14] S. M. Sze, *Physics of Semiconductor Devices*, 2nd ed. New York: Wiley, 1981, pp. 403–404.

[15] C. C. Ho and B. S. Chiou, "Effects of plasma treatment on the high frequency characteristics of Cu/Ta/hhydrogen silsesquioxane (HSQ) system and electrical behaviors of Cu/Ta/HSQ/Pt MIM capacitors," *Microelectron. Eng.*, vol. 84, no. 4, pp. 646–652, Apr. 2007.

[16] Y. B. Lin and J. Y. M. Lee, "The temperature dependence of the conduction current in $Ba_{0.5}Sr_{0.5}TiO_3$ thin-film capacitors for memory device applications," *J. Appl. Phys.*, vol. 87, no. 4, pp. 1941–1843, Feb. 2000.

[17] K. H. Allers, "Prediction of dielectric reliability from I–V characteristics: Poole–Frenkel conduction mechanism leading to root E model for silicon nitride MIM capacitor," *Microelectron. Reliab.*, vol. 44, no. 3, pp. 411–423, Mar. 2004.

[18] S. Ezhilvalavan and T.Y. Tseng, "Electrical properties of Ta_2O_5 thin films deposited on Cu," *Thin Solid Films*, vol. 360, no. 1–2, pp. 268–273, Feb. 2000.

Chia-Cheng Ho (S'08) received the B.S. and M.S. degrees in electronic engineering in 2000 and 2002, respectively, from National Chiao-Tung University, Hsinchu, Taiwan, R.O.C., where he is currently working toward the Ph.D. degree in electrical institute.

From 2007 to 2008, he was a Visiting Assistant in Research (VAR) at Yale University, where he was engaged in the development and simulation of the inelastic electron tunneling spectroscopy (IETS). His current research interests include high k material, nano device, and high frequency circuit.

Bi-Shiou Chiou (M'99–SM'03) received the B.S. degree in nuclear engineering and the M.S. degree in health physics, both from the National Tsing Huang University, Hsinchu, Taiwan, R.O.C., in 1975 and 1977, respectively, and the Ph.D. degree in materials science and engineering from Purdue University, West Lafayette, IN, in 1981.

She is currently a Professor of electronics engineering at the National Chiao-Tung University, Hsinchu. Her current research interests include electronic packaging, electronic ceramics, thick and thin film technology, nano technology, and optoelectronic packaging.

Li-Chun Chang received the B.E. and M.E. degrees in materials science and engineering from National Cheng Kung University, Tainan, Taiwan, R.O.C., in 1990 and 1992, and the Ph.D. degree in electronics engineering from National Chiao-Tung University, Hsinchu, Taiwan, R.O.C., in 2005.

During 2005 to 2007, she was an Assistant Professor at Huafan University, Taipei, Taiwan. She is currently an Assistant Professor at Mingchi University of Technology, Taipei. Her current research interests include resistive random access memory (RRAM) and electronic ceramics.